The nature of the hole traps in reoxidized nitrided oxide gate dielectrics

A. Mallik, J. Vasi, and A. N. Chandorkar

Citation: Journal of Applied Physics **74**, 2665 (1993); doi: 10.1063/1.354658
View online: http://dx.doi.org/10.1063/1.354658
View Table of Contents: http://scitation.aip.org/content/aip/journal/jap/74/4?ver=pdfcov
Published by the AIP Publishing

The nature of the hole traps in reoxidized nitrided oxide gate dielectrics

A. Mallik, J. Vasi, and A. N. Chandorkar
Department of Electrical Engineering, Indian Institute of Technology, Bombay 400 076, India

(Received 16 December 1992; accepted for publication 7 May 1993)

To find out the nature of hole traps in reoxidized nitrided oxide (RNO), a series of field and thermal detrapping experiments were performed following irradiation. It has been found that not only are the hole traps in RNO located near the gate-SiO_2 interface instead of near the Si-SiO_2 interface as in conventional dry oxides, but that the energy distribution of these traps is also quite different from that in conventional oxides. This indicates that the origin of the traps in RNO is different from that normally found in conventional oxides.

INTRODUCTION

In the last several years, nitrided oxides (NO) and reoxidized nitrided oxides (RNO) have evinced a lot of interest because of higher dielectric strength, improved barrier against diffusion of impurities and contaminants, improved resistance under electrical stress, and improved radiation resistance as compared to conventional oxides.[1–21] Though the presence of a large number of electron traps in NO limits its application,[21,22] these traps are significantly reduced in RNO making it attractive for very large scale integration (VLSI) as well as for space applications.

Though there have been numerous publications over the last few years to demonstrate the improved radiation performance of RNO as compared to conventional (dry) oxides, very little effort has been made to find out why RNO behaves differently. Biased irradiation experiments and etch-off experiments[20] suggest that the location of the hole traps in RNO is near the gate-SiO_2 interface instead of near the Si-SiO_2 interface as in conventional oxides. Based on the field detrapping experiments following irradiation, Dunn *et al.*[19] speculated that the nature of the dominant hole traps in RNO is different from the hole traps normally found in conventional oxides. In this paper we report an investigation of the nature of the hole traps in RNO by performing a series of field and thermal detrapping experiments following irradiation. We observed that not only are the hole traps located near the gate-SiO_2 interface in RNO, but also that the activation energy distribution of these hole traps is different from that in conventional oxides. Our finding is consistent with recent electron spin resonance study of the defects in RNO[23,24] which report that the dominant hole traps in RNO is not the well-known E' center as in conventional oxides.

EXPERIMENTAL

The metal-oxide-semiconductor (MOS) capacitors used for this study were fabricated on 0.8–1.2 Ω cm boron-doped (100) silicon wafers. For the RNO devices, initial oxidation was done at 1000 °C in pure oxygen followed by nitridation at 1050 °C in ammonia for 20 min followed by reoxidation at 1050 °C for 75 min in pure oxygen followed by post-reoxidation annealing for 25 min at the reoxidation temperature. This was the optimum processing condition with respect to radiation performance.[25] Oxidation for control (dry) oxide devices was done at 1000 °C in pure oxygen followed by post-oxidation annealing in nitrogen for 25 min at the same temperature. The thickness of the oxide was 36 nm in both cases. Aluminum was deposited by *e*-beam evaporation through a metal mask defining the gate electrodes. Finally, all the devices received a forming gas anneal at 450 °C for 30 min.

High-frequency CV was used to characterize the MOS capacitors before and after irradiation and after various field/thermal annealing cycles following irradiation. Irradiation was performed using a ^{60}Co gamma-ray source with a dose rate of 300 krad (Si)/hour. All detrapping experiments were performed following irradiation of 1 Mrad (Si) of radiation dose.

RESULTS AND DISCUSSIONS

The pre-irradiation values of midgap voltage (V_{mg}) were −0.33 and −1.02 V for control oxide devices and RNO devices, respectively. The RNO devices are known to have more fixed oxide charge than conventional oxide devices which results in less initial V_{mg} for RNO devices.

The devices were irradiated without bias up to a dose of 1 Mrad (Si). The shifts in V_{mg} for 1 Mrad (Si) radiation dose were −0.49 and −1.06 V, respectively, for the RNO and control oxide devices. Soon after the irradiation, the devices were kept at zero bias for 1 h at room temperature. Then one set of devices was subjected to progressively higher positive gate bias starting from 4 V with a step of 4 V. Another set of devices was subjected to progressively higher negative gate bias starting from −4 V with a step of −4 V. At each bias condition, the devices were kept for 1 h. After each bias, the change in V_{mg} was monitored. The unannealed fraction N, which is a measure of annealing of the radiation damage, is defined as

$$N=\frac{\Delta V_{mg}(t)}{\Delta V_{mg}(0)}, \tag{1}$$

where $\Delta V_{mg}(0)$ is the radiation-induced midgap-voltage shift and $\Delta V_{mg}(t)$ is the midgap-voltage shift after any annealing cycle following irradiation, both measured with respect to the pre-irradiation value of midgap voltage on the same device. Figure 1 shows the plot of unannealed fraction as a function of gate bias for the RNO as well as

 0021-8979/93/74(4)/2665/4/$6.00

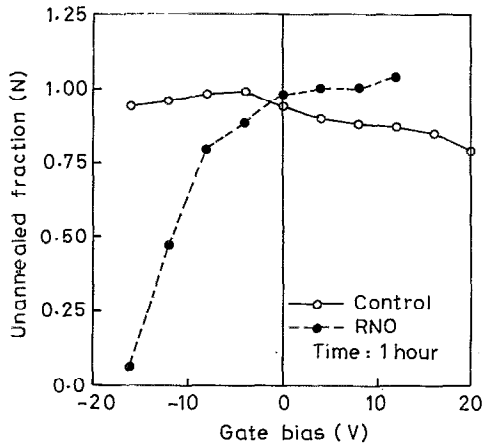

FIG. 1. Field detrapping of the radiation-induced trapped charges in control oxide as well as RNO devices at different gate bias conditions.

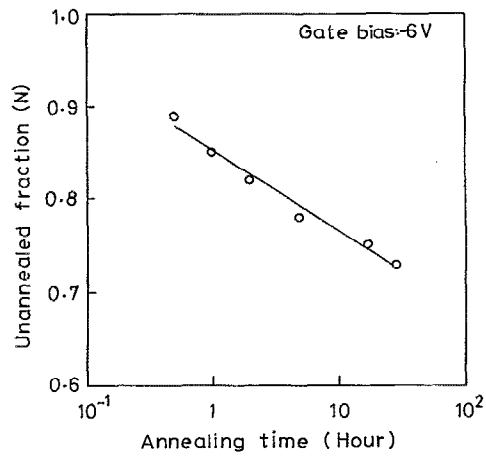

FIG. 3. Field detrapping of the radiation-induced trapped charges in RNO devices.

control oxide devices. As seen from the Fig. 1, for the control oxide devices, the detrapping is only a few percent when negative bias is applied to the gate. With positive bias at the gate, detrapping is somewhat more. The positive bias condition at the gate for the control oxide devices also resulted in skewing in the *CV* curve indicating interface-state generation as expected. On the other hand, for RNO devices with positive bias at the gate, no detrapping is observed and there was no skewing in the *CV* curve. But large negative bias at the gate results in complete detrapping of the trapped charges. This result indicates that the hole traps in RNO are located close to the gate-SiO_2 interface instead of near the Si-SiO_2 as found in conventional oxides consistent with the earlier observations.[19,20]

To find out the detrapping mechanism, the field detrapping experiment was repeated for the RNO devices with constant negative bias applied at the gate. The detrapping of the trapped charges was monitored as a function of time. After irradiation, -6 V was applied to the gate and V_{mg} was measured as a function of time. After 29 h the gate bias was increased to -10 V and after another 30 h the bias was increased to -15 V. As evident in Fig. 2, the unannealed fraction has a tendency to saturate at a particular level at sufficiently long time. The level is different for different gate bias and at a large bias like -15 V, all the trapped charges are detrapped within 2 h. In Fig. 3, the unannealed fraction is plotted against $\ln(t)$ for the -6 V gate bias condition, resulting in a straight line. This indicates that the mechanism of detrapping is tunneling.[26] Increasing the negative bias lowers the trapezoidal tunneling barrier and therefore we see a reduction in the unannealed fraction.

Figure 4 shows the result of an isothermal detrapping experiment following irradiation for RNO as well as control oxide devices. The detrapping was done at 200 °C without bias. The unannealed fraction was monitored as a function of time. As evident from the figure, the RNO devices show a different annealing behavior indicating different activation energy related to the annealing process.

Figure 5 shows the result of isochronal detrapping following irradiation for both RNO and control oxide de-

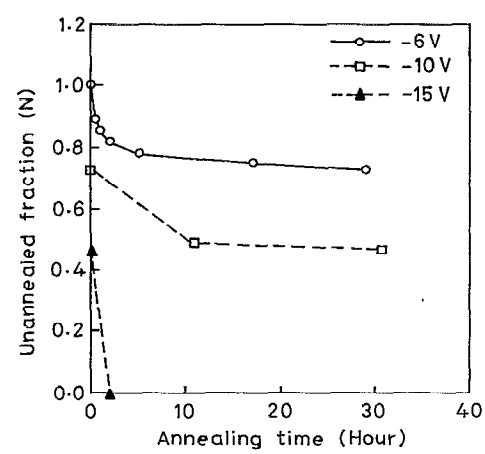

FIG. 2. Field detrapping of the radiation-induced trapped charges in RNO devices as a function of time.

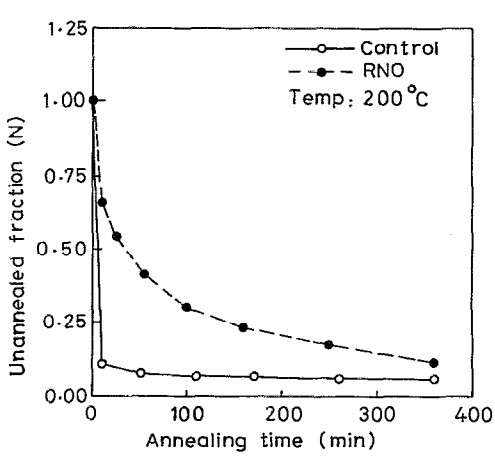

FIG. 4. Isothermal detrapping of the radiation-induced trapped charges in control oxide as well as RNO devices.

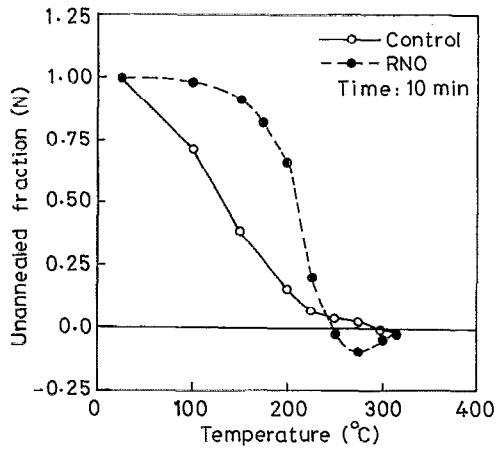

FIG. 5. Isochronal detrapping of the radiation-induced trapped charges in control oxide as well as RNO devices.

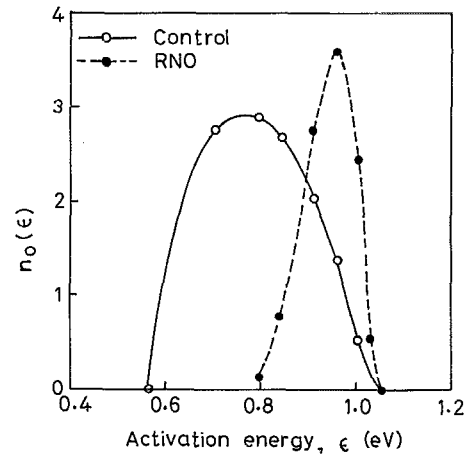

FIG. 6. Activation energy distribution of annealing of the radiation-induced trapped charges in control oxide as well as RNO devices.

vices. After irradiation, the devices were subjected to progressively higher temperature starting from room temperature to 315 °C without bias. At each temperature, the devices were kept for 10 min before HFCV measurement. The greatest change in unannealed fraction, as seen in Fig. 5, takes place between 150 and 250 °C for RNO devices against between 50 and 225 °C for control oxide devices.

It is also seen in Fig. 5 that almost all the trapped holes get detrapped at and above 250 °C. RNO is known to have more electron traps than conventional oxides. In another investigation we have studied the isochronal annealing behavior of the trapped electrons (the electron traps were filled by avalanche injection of electrons) in RNO and found that the unannealed fraction for the trapped electrons is appreciable at 250 °C when almost all the trapped holes get detrapped. During irradiation, because of the higher density of electron traps in RNO, electron trapping does occur in RNO, though it is only about 20% of the hole trapping.[27] As a result, we see that for the RNO devices the unannealed fraction becomes negative, passes through a valley and then comes back to zero as the electron traps also get detrapped at higher temperatures.

Following the derivation of Refs. 28 and 29, the isochronal detrapping data of Fig. 5 have been analyzed for activation energies of the annealing process assuming a first-order reaction kinetics:

$$\frac{dn}{dt} = -Kn, \tag{2}$$

where n is the density which undergoes the annealing process, t is the annealing time, and K is the rate constant which is related to temperature through Arrhenius relation:

$$K = A \exp[-\epsilon/\tau(t)], \tag{3}$$

where τ is the product of Boltzmann constant and temperature and can be a function of time in general, ϵ is the activation energy of the annealing process, and A is the frequency factor.

Substituting Eq. (3) in (2) and integrating we get

$$n(t) = n_0 \exp\left(-A \int_0^t \exp[-\epsilon/\tau(t')]\,dt'\right). \tag{4}$$

For a distribution of energies, Eq. (4) can be written as

$$N(t) = \int_0^\infty n(\epsilon)\,d\epsilon$$

$$= \int_0^\infty n_0(\epsilon) \exp\left(-A \int_0^t \exp[-\epsilon/\tau(t')]\,dt'\right) d\epsilon, \tag{5}$$

where $n_0(\epsilon)$ is the initial energy distribution.

If Eq. (5) is normalized by letting $N(t=0)=1$, then $N(t)$ will correspond directly to the unannealed fraction. Using appropriate approximations, it can be shown[28] that the activation energy ϵ is given by the transcendental equations:

$$\frac{\epsilon}{\tau} + \ln\left(\frac{\epsilon}{\tau} + 2\right) = \ln(Ac\tau), \tag{6}$$

$$n_0(\epsilon) = -\frac{dN}{d\tau}\frac{1}{\epsilon/\tau + 1}, \tag{7}$$

where c is the tempering constant and for our experimental condition the value of c was 2.78×10^5 s/eV.

Equations (6) and (7) were used to analyze the data of Fig. 5. The value of the frequency factor was taken as $10^7\ s^{-1}$. The activation energy distribution is shown in Fig. 6 for both in RNO as well as control oxide devices. The activation energy distribution function was normalized letting $N(t=0)=1$ for the control oxide case. In other words, the area under the curve for the control oxide device would be equal to unity whereas the area under the curve for the RNO device would be equal to $[\Delta V_{mg}(t=0)]_{RNO}/[\Delta V_{mg}(t=0)]_{control}$.

As we see in Fig. 6, the activation energy for the control oxide devices is widely distributed over the energy range of 0.57–1.05 eV. In the case of RNO devices, on the contrary, the distribution is sharp and distributed only

over the energy range of 0.78–1.05 eV with a peak at 0.96 eV. Activation energy distribution is Fig. 6 is a reflection of the results of Fig. 5 because in Fig. 5 we see that the appreciable change in the unannealed fraction takes place sharply over a narrow range of temperature for RNO devices against a much larger range of temperature for the control devices.

The choice of the value of the frequency factor is arbitrary to some extent and therefore the distribution is not uniquely determined on the activation-energy axis. Choosing a frequency factor few orders of magnitude higher would result in only a small translation of the spectra along the activation-energy axis along with a slight broadening of the spectra.[28]

In summary, the field detrapping experiment shows that the dominant hole trap in RNO is located close to the gate-SiO_2 interface instead of close to the Si-SiO_2 interface as normally found in conventional oxides. We have also shown that the mechanism of detrapping is tunneling. Since all the trapped holes get detrapped on the application of appropriate negative gate bias, we conclude that they are located within tunneling distance from the gate-SiO_2 interface. Both the isothermal detrapping and isochronal detrapping experiments show different detrapping behavior of the trapped charges in RNO devices and in control oxide devices. Analysis of the isochronal detrapping data demonstrates that in conventional oxide devices, the activation energy of the trapped holes is widely distributed over the energy range of 0.57–1.05 eV whereas in RNO devices the activation energy distribution is sharper and centered around 0.96 eV. This indicates that the nature of the hole traps in RNO is quite different from that in conventional oxides. In other words, the hole traps which are normally found in conventional oxides are removed in RNO whereas a new type of hole trap is introduced in RNO by the RNO process itself.

Oxides processed at different conditions might have a difference in the nature of the hole traps in them. One important point to note here is that the difference in the nature of the hole traps in our control oxide and RNO is due to the RNO process (i.e., nitridation and reoxidation) and not due to the difference in the initial oxidation or anything else because the control oxide and RNO devices were processed simultaneously in the same batch and the only difference between them was the RNO process.

Our finding is also consistent with the recent electron spin resonance study of defects in RNO which show that the dominant hole traps in RNO is not the well-known E' center as in conventional oxides.[23,24] The microscopic origin of the hole traps in RNO has yet to be identified.

CONCLUSIONS

We performed a series of field and thermal detrapping experiments following irradiation to find out the nature of the hole traps in reoxidized nitrided oxide gate dielectrics. We found that not only are the hole traps located near the gate-SiO_2 interface in RNO instead of near the Si-SiO_2 interface as normally found in conventional oxides, but the activation energy distribution of these traps in RNO is also different from that in conventional oxides. This confirms the speculation that the nature of the hole traps in RNO is quite different from that in conventional oxides. In other words, the hole traps which are normally found in conventional oxides are removed in RNO whereas a new type of hole trap is introduced in RNO by the RNO process itself.

ACKNOWLEDGMENT

The work was funded by the Department of Electronics, Government of India.

[1] T. Ito, T. Nakamura, and H. Ishikawa, IEEE Trans. Electron. Devices **ED-31**, 498 (1984).
[2] F. L. Terry, R. J. Aucoin, M. L. Naiman, and S. D. Senturia, IEEE Electron. Device Lett. **EDL-4**, 191 (1983).
[3] R. K. Pancholy and F. M. Erdmann, IEEE Trans. Nucl. Sci. **NS-30**, 4141 (1983).
[4] G. A. Ruggles and J. R. Monkowski, J. Electrochem. Soc. **133**, 787 (1986).
[5] R. Sundaresan, M. M. Matloubian, and W. E. Bailey, IEEE Trans. Nucl. Sci. **NS-33**, 1223 (1986).
[6] K. S. Krisch, B. J. Gross, and C. G. Sodini, J. Appl. Phys. **70**, 2185 (1991).
[7] G. J. Dunn and S. A. Scott, IEEE Trans. Electron. Devices **ED-37**, 1719 (1990).
[8] Z. H. Liu, P. T. Lai, and Y. C. Cheng, IEEE Trans. Electron. Devices **ED-38**, 334 (1991).
[9] W. Yang, R. Jayaraman, and C. G. Sodini, IEEE Trans. Electron. Devices **ED-35**, 935 (1988).
[10] Z. H. Liu, P. S. Chen, Y. C. Cheng, and P. T. Lai, J. Electrochem. Soc. **137**, 1871 (1990).
[11] Z. J. Ma, Z. H. Liu, P. T. Lai, S. Fleischer, and Y. C. Cheng, Solid-State Electron. **35**, 95 (1992).
[12] Z. H. Liu, P. T. Lai, and Y. C. Cheng, IEEE Trans. Electron. Devices **ED-38**, 344 (1991).
[13] G. J. Dunn and J. T. Krick, IEEE Trans. Electron. Devices **ED-38**, 901 (1991).
[14] B. S. Doyle and G. J. Dunn, IEEE Electron. Dev. Lett. **EDL-12**, 63 (1991).
[15] D. K. Shih, D. L. Kwong, and S. Lee, Appl. Phys. Lett. **54**, 822 (1989).
[16] P. J. Wright, A. Kermani, and K. C. Saraswat, IEEE Trans. Electron. Devices **ED-37**, 1836 (1990).
[17] G. Q. Lo, W. C. Ting, and D. L. Kwong, Appl. Phys. Lett. **56**, 2548 (1990).
[18] G. J. Dunn, B. J. Gross, and C. G. Sodini, IEEE Trans. Electron Devices **ED-39**, 677 (1992).
[19] G. J. Dunn and P. W. Wyatt, IEEE Trans. Nucl. Sci. **NS-36**, 2161 (1989).
[20] G. J. Dunn, J. Appl. Phys. **65**, 4879 (1989).
[21] T. Hori, H. Iwasaki, and K. Tsuji, IEEE Trans. Electron. Devices **ED-35**, 904 (1988).
[22] K. Ramesh, A. N. Chandorkar, and J. Vasi, J. Appl. Phys. **65**, 3958 (1989).
[23] I. A. Chaiyasena, P. M. Lenahan, and G. J. Dunn, J. Appl. Phys. **72**, 820 (1992).
[24] J. T. Yount, P. M. Lenahan, and G. J. Dunn, IEEE Trans. Nucl. Sci. **39**, 2211 (1992).
[25] N. Bhat, Electrical Engineering M. Tech. dissertation, I. I. T. Bombay, India, 1992.
[26] S. Manzini and A. Modelli, in *Insulating Films on Semiconductors*, edited by J. F. Verweij and D. R. Wolters (North-Holland, New York, 1983), p. 112.
[27] A. Mallik, J. Vasi, and A. N. Chandorkar (unpublished).
[28] V. Danchenko, U. D. Desai, and S. S. Brashears, J. Appl. Phys. **39**, 2417 (1968).
[29] V. Danchenko, E. G. Stassinopoulos, P. H. Fang, and S. S. Brashears, IEEE Trans. Nucl. Sci. **NS-27**, 1658 (1980).